VNU Journal of Science: Mathematics – Physics, Vol. 37, No. 2 (2021) 22-30

VNU Journal of Science: Mathematics - Physics

Journal homepage: https://js.vnu.edu.vn/MaP

Original Article

Energy Level Locations of Lanthanide Ions in Strontium-Aluminosilicate Phosphors

Ho Van Tuyen*, Nguyen Ha Vi

Duy Tan University, 3 Quang Trung, Hai Chau, Da Nang, Vietnam

Received 05 August 2020
Revised 29 August 2020; Accepted 15 September 2020

Abstract: This paper determines the position of energy levels of lanthanide ions in $Sr_2Al_2SiO_7$ (SAS) phosphor by a combining analysis of the lowest 4f-5d transition of Ce^{3+} ions and the charge transfer of Eu^{3+} ions-doped SAS phosphor. The SAS samples were successfully synthesized via solid state reaction, and their structure phase was further confirmed by X-ray diffraction. In the case of Eu^{3+}-doped SAS phosphors, the energy of the charge transfer (CT) transition of the Eu^{3+} is about 4.70 eV (264 nm) and this energy is applied to determine the position 4f level of all divalent lanthanides relating to the top of the valence band in the SAS host lattice. For Ce^{3+} activated SAS samples, the lowest $4f^1 \rightarrow 4f^0 5d^1$ excitation energy is determined around 3.71 eV (334 nm) and it is used to estimate the lowest 4f-5d transitions for all lanthanide (Ln) ions in host lattice. A broad band emission of the 5d→4f transition of Ce^{3+} ions includes two peaks emission with different energy about 1997 cm^{-1} that coincides with the theoretical value of 2000 cm^{-1}. The host referred binding energy (HRBE) diagram of all Ln^{2+} and Ln^{3+} ions relating to the valance band of SAS materials has been constructed by using the data of fluorescent properties of Ce^{3+} and Eu^{3+} ions. The energy of 4f→5d transitions of Eu^{2+} ions that was predicted from the energy level scheme matches well with the observed experimental energy.

Keywords: Charge transfer, lanthanide, cerium, europium, energy levels

1. Introduction

The last decade has brought along the increased interests in new solid state luminescent materials, among which, lanthanides (Ln) doped strontium aluminosilicate, $Sr_2Al_2SiO_7$ (SAS), phosphors have attracted the attention of scientists in recent years because of their advantage as highly thermal stable

*Corresponding author.
Email address: hovantuyen@gmail.com

https//doi.org/ 10.25073/2588-1124/vnumap.4594

[1], steady crystalline structure [2]. In some recent studies, Eu^{2+}-doped SAS materials have been synthesized to obtain green emission phosphor [3]; long persistent luminescence and thermoluminescence properties of Eu and Ln^{3+} (Dy^{3+}, Ce^{3+}, Tm^{3+}) co-doped into SAS host materials have also reported [4-8]; Energy transfer between Ce^{3+} and Dy^{3+}, Eu^{3+} ions as well as the concentration quenching of Ce^{3+} in SAS materials have been studied [9-11]. Besides that, the fabrication method for SAS phosphors has been studied and reported in several papers [12, 13] and some other studies have focused on the controllable photoluminescence or thermal stablility of the prepared materials [1, 14].

It is known that, in different host lattices, the emission color and the thermal stability of luminescence materials are very various and these aspects are related to the position of energy levels of lanthanide ions in host lattice [15-17]. From information of the energy level position of a Ln ion in a compound, it will predict some luminescent and thermoluminescence properties of Ln ions in a compound. As presented above, many Ln ions were activated in SAS lattice to estimate the performance of their luminescent characteristic. However, there has been no literature until now presenting the position of Ln ions in the SAS host lattice. Therefore, in this study, the host referred binding energy (HRBE) diagram for all lanthanide ions in the SAS host lattice will be constructed and used to explain the nature emission of Ln ions doping this host material.

2. Experimental

The sample $Sr_2Al_2SiO_7:Ce^{3+}$ (1 mol%) and $Sr_2Al_2SiO_7:Eu^{3+}$ (1 mol%) were fabricated by solid-state reaction method at high temperature. Firstly, the raw materials, $SrCO_3$ (AR), Al_2O_3 (AR), SiO_2 (Sigma), Ce_2O_3 (Merck), and Eu_2O_3 (Merck) were weighted according to the nominal composition, mixed homogeneously and milled thoroughly using an agate pestle and mortar to achieve a uniform mixture. A small amount of B_2O_3 was added during mixing process to serve as a flux to promote the formation of crystal structure. After that, this mixture was ground and calcined at 1250°C for 2 h in air. To obtain the $Sr_2Al_2SiO_7:Eu^{2+}$ phosphor, the obtained $Sr_2Al_2SiO_7:Eu^{3+}$ sample after calcination at 1250°C was further annealed in the reduction atmosphere at 900°C for 1 h. The obtained product was finally ground into powder to analyze phase compositions and luminescent property.

Structural characteristic of the prepared samples was investigated by X-ray diffraction (XRD) patterns using an X-ray diffractometer D8-Advance (Bruker, Germany). The surface homology of the prepared samples was examined with a scanning electron microscope (SEM) (Jeol 6490, JED 2300; Japan). Photoluminescence (PL) and photoluminescence excitation (PLE) spectra were taken out by a spectrophotometer (FL3-22, Horiba Jobin-Yvon).

3. Results and Discussion

3.1. X-ray Diffraction and SEM Image

X-ray diffraction (XRD) patterns of the as-prepared samples $Sr_2Al_2SiO_7:Ce^{3+}$ (SASC) and $Sr_2Al_2SiO_7:Eu^{3+}$ (SASE) were figured out by using Cu K-alpha (0.154 nm) radiation and their results are presented in Figure 1. The strong diffraction peaks are in accordance with those of tetragonal phase (JCPDS: 38-1333). No impure phases were found indicating that the single phase $Sr_2Al_2SiO_7$ was successfully synthesized with used technology conditions. The crystal structure of the prepared materials $Sr_2Al_2SiO_7$ can be refined to be tetragonal, space group P421m with lattice parameters (a=7.820 Å, b=7.820 Å, and c=5.264 Å). SEM images of two prepared samples presented Figure 2 are similar in

shape and size. It can be seen that the particles tend to agglomerate, forming clusters with irregular shapes and a large size.

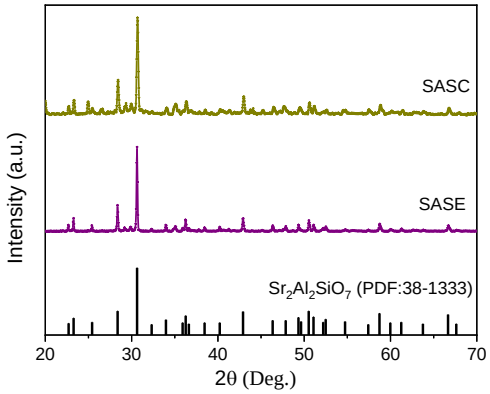

Figure 1. XRD patterns of SASC and SASE samples.

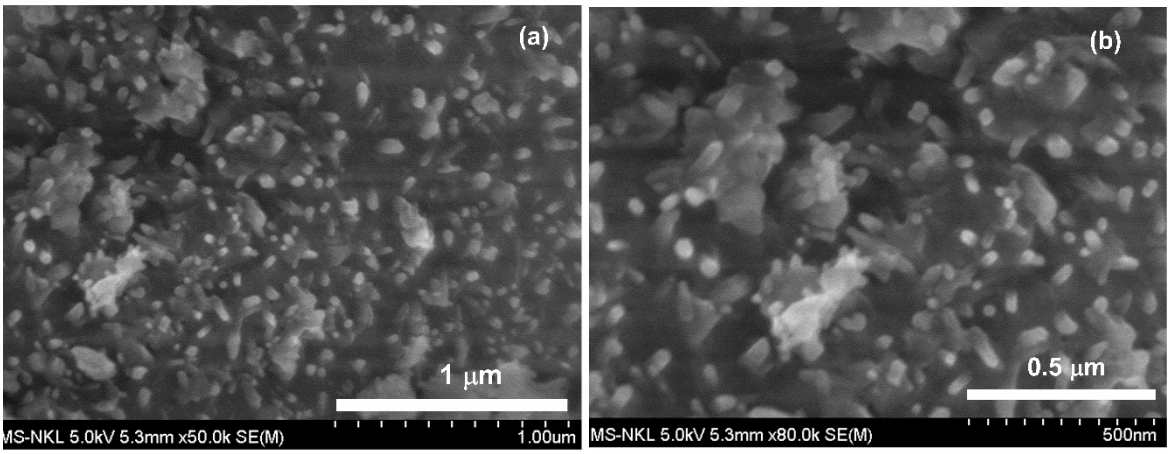

Figure 2. SEM images of SASC (a) and SASE (b) samples

3.2. Luminescent Properties of SASC and SASE Phosphors

Figure 3 illustrates photoluminescence excitation (PLE) and photoluminescence (PL) spectra of SASC sample at room temperature. The PL spectrum was measured under excitation wavelength of 334 nm and it shows a broad-band emission centered at 400 nm, which is caused by the 5d→4f transition of Ce^{3+} ions. This emission band also shows asymmetry that results from the spin-orbit coupling into two levels ($^2F_{5/2}$ and $^2F_{7/2}$) of the 4f ground state of the Ce^{3+} ions [18, 19], and it can be deconvoluted into two Gaussians peaking at 396 nm (3.13 eV) and 430 nm (2.88 eV). The energy difference between the spin-orbit spliting of the 4f ground state in the SASC sample is about 1997 cm^{-1}, which is in good agreement with the general value 2000 cm^{-1} [19, 20].

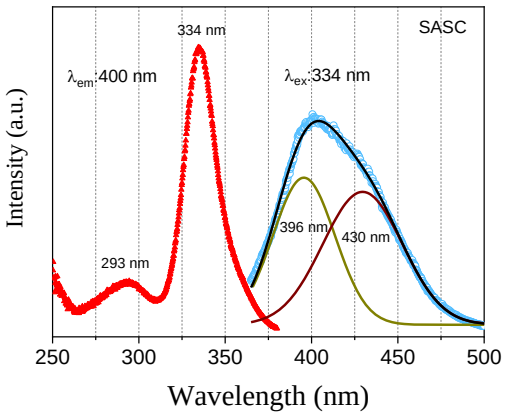

Figure 3. PLE and PL spectra of SASC sample.

The PLE spectrum of SASC sample recorded at the emission wavelenght of 400 nm shows two broad bands centered at 334 nm and 293 nm, which are the excited transitions from the 4f ground state to the $5d_J$ excited states of the Ce^{3+} ions. In which the broad band peaking at 334 nm (3.71 eV) is identified to the lowest $4f^1 \rightarrow 5d^1$ excitation transition (arrow 1 in Figure 5) of the Ce^{3+} ions in the SAS host lattice, and this energy is one of the parameters to construct the energy level scheme of the lanthanide levels in SAS host lattice in the next section.

PL spectrum under the excitation wavelength of 393 nm and PLE spectrum recorded at emission wavelength of 617 nm of SASE sample at room temperature are presented in Figure 4. The PL spectrum includes five strong peaks locating at 576 nm ($^5D_0 \rightarrow {}^7F_0$), 586 nm ($^5D_0 \rightarrow {}^7F_1$), 617 nm ($^5D_0 \rightarrow {}^7F_2$), 655 nm ($^5D_0 \rightarrow {}^7F_3$), and 700 nm ($^5D_0 \rightarrow {}^7F_4$). The sample exhibits the red emission with the main contribution of the $^5D_0 \rightarrow {}^7F_2$ transition. The PLE spectrum recorded in the 240-550 nm region has a broad band at 240-325 nm and many sharp peaks in the 325-550 nm region. The intense sharp peaks include the $^7F_{0/1} \rightarrow {}^5D_1$ transitions (524 nm), the $^7F_0 \rightarrow {}^5D_2$ transition (462 nm), the $^7F_0 \rightarrow {}^5L_6$ transition (393 nm), and the $^7F_0 \rightarrow {}^5D_4$ transition (361 nm), which correspond to the excited transitions of electrons from the ^7F_J levels to the excited levels of Eu^{3+} ions in SAS compound, while the broad band with maximum at 264 nm is the charge transfer (CT) transition between the Eu^{3+} ions and host lattice. Energy of this CT band (E^{CT}) is 4.70 eV; it is also used to construct the energy level diagram of lanthanide ions in SAS host lattice in Section 3.3.

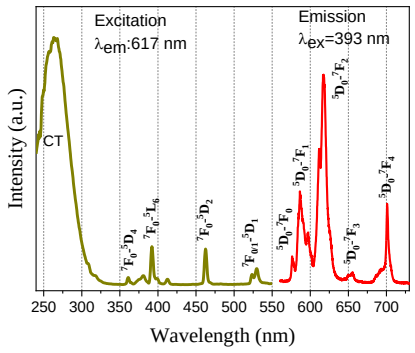

Figure 4. PLE and PL of SASE sample.

3.3. Construction of the Energy Level Scheme of Lanthanides in the SAS Host Lattice

In this section, the host referred binding energy (HRBE) diagram for all lanthanide ions in the SAS host lattice will be constructed by using energies of the lowest 4f-5d transition of Ce^{3+} ions and the charge transfer of Eu^{3+} ions in this material.

Firstly, the lowest 4f-5d energies $E_{fd}(Ln^{3+/2+}, SAS)$ of the corresponding $Ln^{3+/2+}$ ions in SAS host lattice are predicted from the data of PLE spectrum of Ce^{3+} ions in SASC sample. It is known that in $Ln^{3+/2+}$ ions doped SAS material, $E_{fd}(Ln^{3+/2+}, SAS)$, energies are shifted toward the low energy (redshift) in the comparison with those of corresponding $Ln^{3+/2+}$ free ions. This redshift energy $D(Ln^{3+/2+}, SAS)$ does not change for all lanthanide ions in the same compound but it is affected by the compound. The redshift value relates to the $E_{fd}(Ln^{3+/2+}, SAS)$ as in the following equation [21, 22]:

$$E_{fd}(Ln^{3+/2+}, SAS) = E_{fd}(Ln^{3+/2+}, free) - D(Ln^{3+/2+}, SAS) \quad (1)$$

where $E_{fd}(Ln^{3+/2+}, free)$ is the energy of the lowest 4f→5d excited state of free $Ln^{3+/2+}$ ions and its values for all lanthanides have been found in the literature [23]. In Section 3.2, $E_{fd}(Ce^{3+}, SAS)$ is found to be 3.71 eV (334 nm) from PLE spectrum of SASC sample in Figure 3. Therefore, $D(Ln^{3+}, SAS)$ value is determined by using the known $E_{fd}(Ce^{3+}, SAS)$ and $E_{fd}(Ce^{3+}, free)$ values, and $D(Ln^{3+}, SAS)$ is found to be 2.41 eV. From this energy, we can predict the $E_{fd}(Ln^{3+}, SAS)$ energies for all Ln^{3+} ions in the SAS host lattice by using Equation 1, and the results are shown in Column 4, Table 1. Besides that, the redshift energies of Ln^{3+} and Ln^{2+} relate to each other as below [21]:

$$D(Ln^{2+}, SAS) = 0.64\, D(Ln^{3+}, SAS) - 0.233 \text{ eV} \quad (2)$$

Using Equation 2, $D(Ln^{2+}, SAS)$ value reaches 1.31 eV and it is used to estimate $E_{fd}(Ln^{2+}, SAS)$ energies for all Ln^{2+} ions in SAS compound via Equation 1. The obtained $E_{fd}(Ln^{2+}, SAS)$ energies are listed in Column 7, Table 1.

Secondly, the energy level positions of the 4f states of Ln^{3+} ions compared to the top of the valence band of SAS compound can be obtained through the charge transfer energy of Eu^{3+} in the same compound. The energy needed to transfer an electron from the valence band to a trivalent lanthanide impurity in a compound is called the charge transfer energy E^{CT}. The E^{CT} value of a trivalent lanthanide ion provides information on the locations of the ground state of the corresponding divalent lanthanide ion relative to the top of the valence band in the same compound, $E^{CT}(Ln^{3+}, SAS) = E_{Vf}(Ln^{2+}, SAS)$ [17, 22, 24]. Among lanthanide ions, Eu^{3+} ion is often used to calculate the E^{CT} value because it has the low charge transfer energy and therefore the E^{CT} value is easy determined from its excitation spectrum. From PLE spectrum of SASE in Figure 4, $E^{CT}(Eu^{3+}, SAS)$ is found of 4.70 eV, hence we obtain the $E_{Vf}(Eu^{2+}, SAS) = 4.70$ eV (arrow 2 in Figure 5). This energy is used to predict $E_{Vf}(Ln^{2+}, CAS)$ for all other divalent lanthanides in the SAS host lattice by using the known energy difference $\Delta E_{Vf}(Ln^{2+}, Eu^{2+})$ in ref. [23] and the results are listed in Column 3, Table 1. For trivalent lanthanides, energy $E_{Vf}(Ln^{3+})$ can be determined via the E^{CT} energy of tetravalent lanthanide (Ln^{4+}) ions. However, there is too little available information on such transitions of the Ln^{4+} ions in literature. Instead, $E_{Vf}(Ln^{3+})$ can be evaluated by using the correlation energy $U(6)$, which is known as the energy difference between the ground state energy of Eu^{2+} and that of Eu^{3+} ions in the same compound [21].

$$U(6, SAS) = E_{Vf}(Eu^{2+}, SAS) - E_{Vf}(Eu^{3+}, SAS) \quad (3)$$

Studies of Dorenbos show that $U(6)$ reaches various values depending the host lattice and it ranges from 6.4 to 7.2 eV in oxide [22]. Some oxide materials get $U(6)$ with the medium value, such as $Y_3Al_5O_{12}$ (6.75 eV) [22] and $Gd_5Si_3O_{12}N$ (6.80 eV) [25]. $Sr_2Al_2SiO_7$ compound is also an oxide host containing silicate, therefore $U(6, SAS)$ is chosen about 6.80 eV. Using Equation 3, $E_{Vf}(Eu^{3+}, SAS)$ is found to be -2.10 eV. It can now predict $E_{Vf}(Ln^{3+}, SAS)$ energies for all trivalent lanthanides in SAS host lattice by

using the known $E_{Vf}(Eu^{3+}, SAS)$ value and the energy difference between the 4f ground state of Ln^{3+} ions with that of Eu^{3+} $\Delta E_{Vf}(Ln^{3+}, Eu^{3+})$ given in [23], the results are listed in Column 6, able 1.

Table 1. Charge transfer energies ($E^{CT} \equiv E_{Vf}$), the lowest 4f→5d energies (E_{fd}) and energies from 5d state to the top of the valence band (E_{5d}) for Ln^{3+} and Ln^{2+} ions in SAS host lattice (all energies are in eV). *n* is the number of electrons in the 4f configuration in trivalent lanthanides

Ln	*n*	$E_{Vf}(Ln^{2+},SAS)$	$E_{fd}(Ln^{2+},SAS)$	$E_{5d}(Ln^{2+},SAS)$	$E_{Vf}(Ln^{3+},SAS)$	$E_{fd}(Ln^{3+},SAS)$	$E_{5d}(Ln^{3+},SAS)$
La	0	10.31	-2.25	8.06	…	…	…
Ce	1	8.83	-0.93	7.90	3.14	3.71	6.85
Pr	2	7.57	0.28	7.85	1.29	5.22	6.51
Nd	3	7.22	0.56	7.78	-0.20	6.51	6.31
Pm	4	7.04	0.65	7.69	-0.64	6.83	6.19
Sm	5	5.95	1.69	7.64	-0.83	6.93	6.10
Eu	6	4.70	2.91	7.61	-2.10	8.09	5.99
Gd	7	9.26	-1.51	7.75	-3.44	9.39	5.95
Tb	8	7.91	-0.12	7.79	1.47	5.37	6.84
Dy	9	6.97	0.86	7.83	0.05	6.84	6.89
Ho	10	6.70	0.94	7.64	-1.05	7.69	6.64
Er	11	7.28	0.81	8.09	-0.98	7.45	6.47
Tm	12	6.42	1.64	8.06	-0.82	7.34	6.52
Yb	13	5.13	2.91	8.04	-1.87	8.48	6.61
Lu	14	…	…	…	-3.11	9.85	6.74

After $E_{Vf}(Ln^{3+/2+}, SAS)$ and $E_{fd}(Ln^{3+/2+}, SAS)$ are determined, the position of the 5d state for all trivalent and divalent lanthanides in SAS host lattice is found by the following expression:

$$E_{5d}(Ln^{3+/2+}, SAS) = E_{Vf}(Ln^{3+/2+}, SAS) + E_{fd}(Ln^{3+/2+}, SAS) \quad (4)$$

The results of E_{5d} for all divalent and trivalent lanthanides are presented in Columns 5 and 8, Table 1, respectively. Using E_{Vf}, E_{5d} in Table 1 and band gap ~5.3 eV [26], we can construct the HRBE diagram for all lanthanide ions in the SAS compound as in Figure 5.

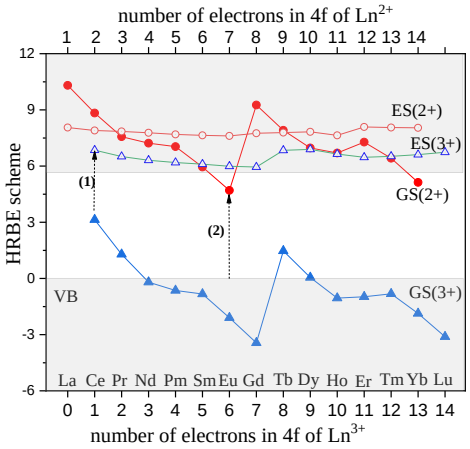

Figure 5. The HRBE scheme of Ln^{2+} and Ln^{3+} ions in SAS host lattice.

To check the correctness of the obtained energy diagram, PL and PLE spectra of Eu^{2+} ions in SAS have been measured to compare to the predicted data from HRBE diagram. The PL spectrum of Eu^{2+}

ions under the excited radiation of 424 nm, shown in Figure 6 (a), has a broad band emission from 450 nm to 650 nm corresponding to the 5d-4f transition of Eu^{2+} ions in SAS host lattice. The PLE spectrum recorded at emission wavelength of 510 nm is presented in Figure 6 (b). It can be seen that the excitation spectrum is a broad band in the 260 - 460 nm region, which is contituted of four 4f-5d excited transitions located 293 nm, 317 nm, 363 nm and 424 nm, in which, the excitation peak at 424 nm (2.924 eV) is the lowest 4f-5d excited transition of Eu^{2+} ions in SAS material and coincides with the result of the excitation spectra of Eu^{2+} ions in ref. [5], which shows the lowest 4f-5d of Eu^{2+} ions is about 425 nm. From the HRBE diagram in Figure 5 and results in Table 1, the predicted lowest 4f-5d of Eu^{2+} ions doped SAS compound is around 2.91 eV and this energy coincides well with the experimental energy in Figure 6 (b) with a slight difference of 0.5%. This indicates that the obtained energy scheme can be used to predict the energy levels positions of lanthanides doped SAS host lattice. Besides, the predicted value of the 4f-5d excited transition of Eu^{2+} ions in Table 1 is 2.91 eV, which coincides with the 5d-4f emission energy of Ce^{3+} ions (2.88-3.13 eV) in Figure 3. Therefore, the energy transfer phenomenon can occur between two ions when they codope SAS host lattice; this prediction has also been confirmed in [5].

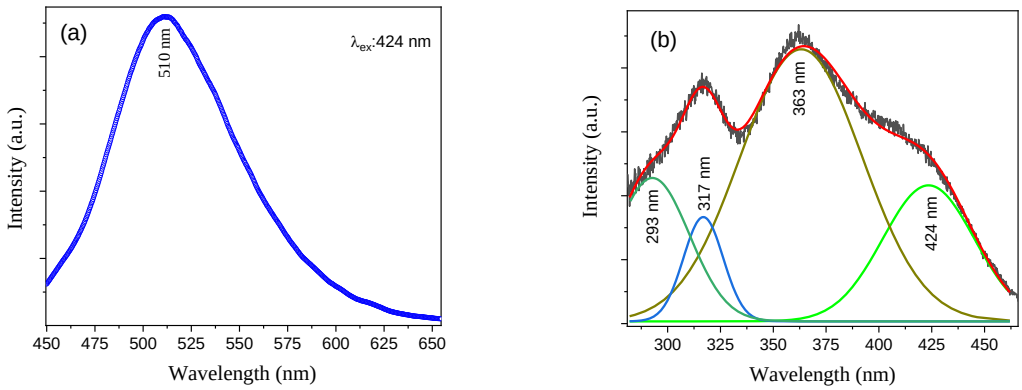

Figure 6. PL (a) and PLE (b) spectra of Eu^{2+} ions doped SAS material.

4. Conclusion

The structure and luminescence properties of $Sr_2Al_2SiO_7$ doped with Eu^{3+} and Ce^{3+} ions (1 mol%) have been studied through X-ray diffraction and fluorescence technique. The energy level positions of Ln^{2+} and Ln^{3+} relative to the valence band in $Sr_2Al_2SiO_7$ host lattice were determined by using data of photoluminescence excitation spectra of Ce^{3+} and Eu^{3+} ions doped $Sr_2Al_2SiO_7$ compound, and the predicted energies from the energy levels scheme were in good agreement with experimental energies.

Acknowledgments

This research is funded by Vietnam National Foundation for Science and Technology Development (NAFOSTED) under Grant 103.03-2018.323.

References

[1] H. Zou, D. Peng, Z. Chu, X. Wang, Y. Li, X. Yao, A Highly Thermal Stable and Waterproof Red Phosphor: Pr^{3+}-doped $Sr_2Al_2SiO_7$, J. Mater. Sci, Vol. 48, No. 22, 2013, pp. 7981-7985, https://doi.org/10.1007/s10853-013-7609-x.

[2] J. Wu, B. Yan, Sol–gel Synthesis of Green-Luminescence Microcrystalline Phosphors $Sr_xCa_{2-x}Al_2SiO_7$:yTb^{3+},zCe^{3+} by Hybrid Precursors, Colloids. Surf. A: Physicochem. Eng. Asp, Vol. 297, No. 3, 2007, pp. 253-257, https://doi.org/10.1016/j.colsurfa.2006.10.052.

[3] F. C. Lu, L. J. Bai, W. Dang, Z. P. Yang, P. Lin, Structure and Photoluminescence of Eu^{2+} Doped $Sr_2Al_2SiO_7$ Cyan-green Emitting Phosphors, ECS J. Solid State Sci. Technol, Vol. 4, No. 2, 2014, pp. R27-R30, https://doi.org/10.1149/2.0151502jss.

[4] Y. Ding, Y. Zhang, Z. Wang, W. Li, D. Mao, H. Han, C. Chang, Photoluminescence of Eu Single Doped and Eu/Dy Codoped $Sr_2Al_2SiO_7$ Phosphors with Long Persistence, J. Lumin, Vol. 129, No. 3, 2009, pp. 294-299, https://doi.org/10.1016/j.jlumin.2008.10.009.

[5] G. Li, M. Li, L. Li, H. Yu, H. Zou, L. Zou, S. Gan, X. Xu, Luminescent Properties of $Sr_2Al_2SiO_7$:Ce^{3+},Eu^{2+} Phosphors for Near UV-excited White Light-emitting Diodes, Mater. Lett, Vol. 65, No. 23, 2011, pp. 3418-3420, https://doi.org/10.1016/j.matlet.2011.07.050.

[6] A. Jadhaw, V. D. Sonwane, A. S. Gour, P. Jha, Thermoluminescence Properties of Eu-doped and Eu/Dy-codoped $Sr_2Al_2SiO_7$ Phosphors, Luminescence, Vol. 32, No. 7, 2017, pp. 1349-1353, https://doi.org/10.1002/bio.3331.

[7] H. Y. Jiao, Y. H. Wang, Intense Red Phosphors for Near-ultraviolet Light-emitting Diodes, Appl. Phys. B, Vol. 98, No. 2, 2009, pp. 423-427, https://doi.org/10.1007/s00340-009-3708-4.

[8] I. P. Sahu, D. P. Bisen, N. Brahme, R. K. Tamrakar, Studies on the Luminescence Properties of Europium Doped Strontium Alumino-silicate Phosphors by Solid State Reaction Method, J. Mater. Sci.: Mater. Electron, Vol. 26, No. 12, 2015, pp. 10075-10086, https://doi.org/10.1007/s10854-015-3691-y.

[9] Y. Gong, Y. Wang, Y. Li, X. Xu, Ce^{3+}, Dy^{3+} Co-doped White-light Long-lasting Phosphor: $Sr_2Al_2SiO_7$ Through Energy Transfer, J. Electrochem. Soc, Vol. 157, No. 6, 2010, pp. J208-J211, https://doi.org/10.1149/1.3371488.

[10] M. Kolte, V. B. Pawade, S. J. Dhoble, Quenching and Dipole–dipole Interactions in $Sr_2Al_2SiO_7$:Ce^{3+} Host Lattice, Appl. Phys. A, Vol. 122, No.2, 2016, pp. 59:1-59:5, https://doi.org/10.1007/s00339-015-9579-0.

[11] H. V. Tuyen, D. T. Tien, N. M. Son, D. V. Phan, Judd–Ofelt Parameters of Eu^{3+} and Energy Transfer of Ce^{3+}/Eu^{3+} in $Sr_2Al_2SiO_7$ Materials, J. Electron. Mater, Vol. 48, No.12, 2019, pp. 7799-7805, https://doi.org/10.1007/s11664-019-07608-6.

[12] W. Pan, G. Ning, Y. Lin, X. Yang, Sol-gel Processed Ce^{3+}, Tb^{3+} Codoped White Emitting Phosphors in $Sr_2Al_2SiO_7$, J. Rare Earth, Vol. 26, No. 2, 2008, pp. 207-210, https://doi.org/10.1016/S1002-0721(08)60066-6.

[13] W. Zhou, X. Ma, M. Zhang, Y. Luo, Z. Xia, Effect of Different RE Dopants on Phosphorescence Properties of $Sr_2Al_2SiO_7$:Eu^{2+} Phosphors, J. Rare Earth, Vol. 33, No. 7, 2015, pp. 700-705, https://doi.org/10.1016/S1002-0721(14)60473-7.

[14] P. Zhang, Z. Lu, Q. Yuan, Q. Hou, T. D. Golden, X. Ren, L. Weng, H. Wang, A Novel Composite Phosphor Via One-pot Synthesis: Single Matrix with Controllable Luminescence, Mater. Chem. Phys, Vol. 134, No. 3, 2012, pp. 1190-1196, https://doi.org/10.1016/j.matchemphys.2012.04.020.

[15] T. Shalapska, P. Dorenbos, A. Gektin, G. Stryganyuk, A. Voloshinovskii, Luminescence Spectroscopy and Energy Level Location of Lanthanide Ions Doped in $La(PO_3)_3$, J. Lumin, Vol. 155, 2014, pp. 95-100, https://doi.org/10.1016/j.jlumin.2014.06.029.

[16] P. Dorenbos, Thermal Quenching of Eu^{2+} 5d–4f Luminescence in Inorganic Compounds, J. Phys.: Condens. Matter, Vol. 17, No. 50, 2005, pp. 8103-8111, https://doi.org/10.1088/0953-8984/17/50/027.

[17] N. N. Trac, H. V. Tuyen, V. X. Quang, M. Nogami, L. V. K. Bao, N. T. Thanh, N. M. Son, N. T. T. An, L. X. Hung, T. T. Hong, Energy Level of Lanthanide Ions and Anomalous Emission of Eu^{2+} in $Sr_3B_2O_6$ Materials, Physica B: Condens. Matter, Vol. 595, 2020, pp. 412373:1-412373:7, https://doi.org/10.1016/j.physb.2020.412373.

[18] Y. Q. Li, N. Hirosaki, R. J. Xie, T. Takeda, M. Mitomo, Yellow-orange-emitting $CaAlSiN_3$:Ce^{3+} Phosphor: Structure, Photoluminescence, and Application in White LEDs, Chem. Mater, Vol. 20, No. 21, 2008, pp. 6704-6714, https://doi.org/10.1021/cm801669x.

[19] A. H. Krumpel, E. van der Kolk, D. Zeelenberg, A. J. J. Bos, K. W. Krämer, P. Dorenbos, Lanthanide 4f-level Location in Lanthanide Doped and Cerium-lanthanide Codoped $NaLaF_4$ by Photo- and Thermoluminescence, J. Appl. Phys, Vol. 104, No. 7, 2008, pp. 073505:1-073505:10, https://doi.org/10.1063/1.2955776.

[20] C. K. Chang, T. M. Chen, $Sr_3B_2O_6:Ce^{3+},Eu^{2+}$: A Potential Single-phased White-emitting Borate Phosphor for Ultraviolet Light-emitting Diodes, Appl. Phys. Lett, Vol. 91, No. 8, 2007, pp. 081902:1-081902:3, https://doi.org/10.1063/1.2772195.

[21] P. Dorenbos, Ce^{3+} 5d-centroid Shift and Vacuum Referred 4f-electron Binding Energies of all Lanthanide Impurities in 150 Different Compounds, J. Lumin, Vol. 135, 2013, pp. 93-104, https://doi.org/10.1016/j.jlumin.2012.09.034.

[22] P. Dorenbos, A Review on How Lanthanide Impurity Levels Change with Chemistry and Structure of Inorganic Compounds, ECS J. Solid State Sci. Technol, Vol. 2, No. 2, 2013, pp. R3001-R3011, https://doi.org/10.1149/2.001302jss.

[23] P. Dorenbos, Charge Transfer Bands in Optical Materials and Related Defect Level Location, Opt. Mater, Vol. 69, 2017, pp. 8-22, https://doi.org/10.1016/j.optmat.2017.03.061.

[24] P. Dorenbos, The Eu^{3+} Charge Transfer Energy and the Relation with the Band Gap of Compounds, J. Lumin, Vol. 111, No. 2, 2005, pp. 89-104, https://doi.org/10.1016/j.jlumin.2004.07.003.

[25] Z. J. Zhang, W. Yang, Luminescence Characteristic of RE (RE = Pr, Sm, Eu, Tb, Dy) and Energy Levels of Lanthanide Ions in $Gd_5Si_3O_{12}N$, Solid State Sci, Vol. 72, 2017, pp. 64-70, https://doi.org/10.1016/j.solidstatesciences.2017.08.015.

[26] Y. Q. Li, N. Hirosaki, R. J. Xie, M. Mitomo, Crystal, Electronic and Luminescence Properties of Eu^{2+}-doped $Sr_2Al_{2-x}Si_{1+x}O_{7-x}N_x$, Sci. Technol. Adv. Mater, Vol. 8, No. 7, 2007, pp. 607-616, https://doi.org/10.1016/j.stam.2007.08.007.